out such a possibility as well and rather points toward some of the other explanations as more likely reasons for tightly bound Pt.

It should be extremely interesting to find out about the role of this firmly bound Pt in the context of the mode of action of Pt antitumor drugs.

Acknowledgment. This work has been supported by the Deutsche Forschungsgemeinschaft, DFG, the Technische Universität, and Degussa (loan of K_2PtCl_4). We thank A. Filippou for assistance with the thermogravimetric study.

Registry No. **1**, 96617-60-6; **2**, 96617-61-7; **3**, 96617-62-8; **4**, 96617-63-9; **5**, 96617-64-0; **6**, 96648-02-1; **7**, 96617-65-1; **8**, 96617-66-2; *cis*-$[(NH_3)_2PtC(Cl)]Cl$, 75659-46-0; *cis*-$[(NH_3)_2PtC_2]Cl_2$, 76123-94-9; *cis*-$[(NH_3)_2PtG_2](NO_3)_2$, 96617-67-3; *cis*-$[(NH_3)_2PtC(OH)](NO_3)$, 80662-76-6; *cis*-$[(NH_3)_2Pt(C\text{-}H)]_2(NO_3)_2$, 75936-23-1; *cis*-$[(NH_3)_2PtG(Cl)]Cl$, 88080-82-4; *cis*-$[(NH_3)_2PtU(H_2O)](NO_3)$, 85715-80-6; *trans*-$(NH_3)_2Pt(CN)_2$, 14523-27-4; *trans*-$(NH_3)_2PtCl_2$, 14913-33-8; $[(NH_3)_4Pt][Pt(CN)_4]$, 14215-56-6; $[(NH_3)_4Pt]Cl_2$, 13933-32-9; *cis*-$[(NH_3)_2Pt(NC)_2Pt(CN)_2]$, 96633-15-7; *cis*-$[(NH_3)_2PtC(H_2O)]^{2+}$, 80662-70-0; *trans*-$[(NH_3)_2PtAC]^{2+}$, 96617-68-4; *trans*-$[(NH_3)_2PtG(Cl)]^+$, 96617-69-5; *trans*-$[(NH_3)_2PtGC]^{2+}$, 96648-03-2; $[(NH_3)_3PtG]^{2+}$, 96617-70-8; *cis*-$[(NH_3)_2PtGC]^{2+}$, 79301-65-8; *trans*-$[(NH_3)PtG_2C]^{2+}$, 96648-85-0; *cis*-$[(NH_3)_2PtUG]^+$, 88005-67-8; *cis*-$[(NH_3)_2PtUC]^+$, 91003-28-0; *cis*-$(NH_3)_2PtCl_2$, 15663-27-1; KCN^-, 57-12-5; *cis*-$(NH_3)_2PtT_2$, 74539-69-8; *cis*-$(NH_3)_2PtU_2$, 83350-97-4; $[Pt(CN)_4]^{2-}$, 15004-88-3.

Contribution from the Department of Chemistry, University of California, Davis, California 95616

Studies of the Chemical Oxidation of Iron(II) Complexes of *N*-Methylporphyrins To Form the Corresponding Iron(III) Complexes

ALAN L. BALCH,* GERD N. LA MAR, LECHOSLAW LATOS-GRAZYNSKI, and MARK W. RENNER

Received February 13, 1985

Oxidation of iron(II) *N*-methylporphyrin halide complexes with chlorine, bromine, or iodine in chloroform solution at −50 °C produces the corresponding iron(III) *N*-methylporphyrin halide cations. The oxidations may be reversed by treating the product solutions with zinc. The iron(III) complexes have been characterized by electronic, ^1H and ^2H NMR, and ESR spectroscopy. The NMR results indicate that the C_s symmetry of the iron(II) parent complexes is retained upon oxidation. Characteristic ^1H NMR shifts for these high-spin ($S = {}^5/_2$) species include the very broad *N*-methyl resonance at ca. 270 ppm (observed only by ^2H NMR), three pyrrole resonances in the 130–75 ppm region and one at ca. 2 ppm, pyrrole methylene resonances in the range 80–20 ppm and meso resonances at ca. −70 ppm. The electronic structure of these iron(III) complexes are similar to those of symmetrical high-spin, five-coordinate iron(III) porphyrins except for the local environment of the methylated pyrrole, which suffers from sharply reduced σ-spin transfer as a consequence of the longer Fe–N distance to that ring. On warming, these iron(III) complexes decompose by demetalation (for chloride complexes) or demethylation (for bromide complexes).

Introduction

The routes to the physiological formation of N-substituted porphyrins have only recently been probed. Substituted hydrazines are known to react with heme proteins to form N-substituted porphyrins,[1,2] and for hemoglobins and myoglobin, there is evidence for the initial formation of (σ-alkyl)- or (σ-aryl)iron(III) porphyrin complexes **1**.[3,4] Studies of model complexes have given insight into the mechanism of transfer of the alkyl or aryl group from iron to the porphyrin. Chemical and electrochemical studies have shown than N-substituted porphyrins **5** are formed from **1** under oxidizing conditions as shown in Scheme I with **2**–**4** as likely intermediates.[4-6]

This paper is concerned with the physical characterization of the iron(III) alkylporphyrin complexes $\mathbf{6^+}$–$\mathbf{10^+}$, formed by chemical oxidation of the air-stable and structurally characterized[7,8] iron(II) halo complexes, **6**–**10**. (i.e. by the second redox step in Scheme I). Particular emphasis is placed on ^1H NMR studies as a source of insight into the electronic structure of these low-symmetry porphyrin species and as a potential means for detecting these complexes in a protein environment. The utility of ^1H NMR studies in the characterization of iron porphyrins has

Scheme I

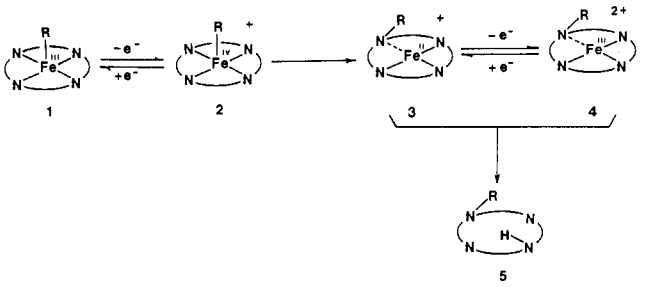

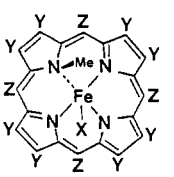

6, Y = H; Z = C_6H_5; X = Cl [(MeTPP)Fe^{II}Cl]
7, Y = H; Z = C_6H_5; X = Br [(MeTPP)Fe^{II}Br]
8, Y = H; Z = *p*-$C_6H_4CH_3$; X = Cl [(MeTpTP)Fe^{II}Cl]
9, Y = C_2H_5; Z = H; X = Cl [(MeOEP)Fe^{II}Cl]
10, Y = C_2H_5; Z = H; X = Br [(MeOEP)Fe^{II}Br]

(1) Saito, S.; Itano, H. A. *Proc. Natl. Acad. Sci. U.S.A.* **1981**, *78*, 5508.
(2) Augusto, G.; Kunze, K. L.; Ortiz de Montellano, P. R. *J. Biol. Chem.* **1982**, *257*, 6231.
(3) Kunze, K. L.; Ortiz de Montellano, P. R. *J. Am. Chem. Soc.* **1983**, *105*, 1380.
(4) Ortiz de Montellano, P. R.; Kunze, K. L.; Augusto, O. *J. Am. Chem. Soc.* **1982**, *104*, 3545.
(5) Mansuy, D.; Battioni, J.-P.; Dupre, D.; Sartori, E.; Chottard, G. *J. Am. Chem. Soc.* **1982**, *104*, 6159.
(6) Lancon, D.; Cocolios, P.; Guilard, R.; Kadish, K. M. *J. Am. Chem. Soc.* **1984**, *106*, 4472.
(7) Anderson, O. P.; Kopelove, A. B.; Lavallee, D. K. *Inorg Chem.* **1980**, *19*, 2101.
(8) Lavallee, D. K. *J. Inorg. Biochem.* **1982**, *16*, 135.

0020-1669/85/1324-2432$01.50/0

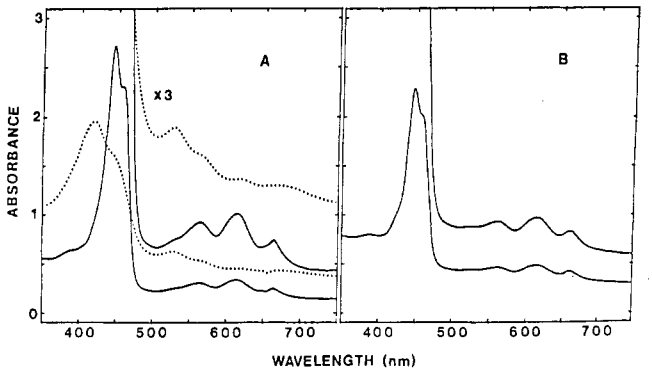

Figure 1. (A) Electronic spectra of chloroform solutions at −60 °C: solid line, 1.6×10^{-4} M (MeTPP)$Fe^{II}Br$ (**6**); dotted line, $[(MeTPP)Fe^{III}Br]^+$ obtained by oxidation of the preceding sample with 1 equiv of bromine. (B) Electronic spectra of the same sample after reduction with zinc and filtration. Cell path length: 1.0 mm.

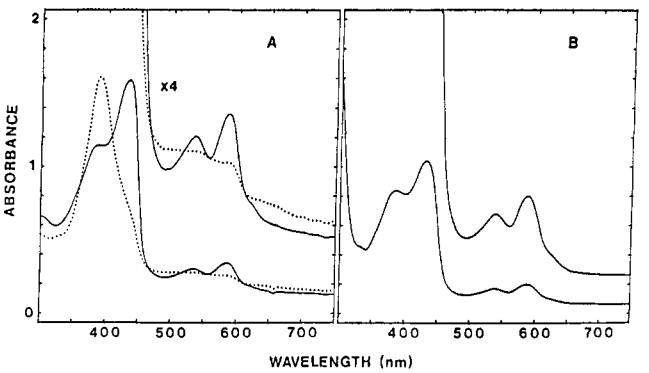

Figure 2. (A) Electronic spectra of chloroform solutions at −60 °C: solid line, 1.8×10^{-4} M (MeOEP)$Fe^{II}Br$ (**10**); dotted line, $[(MeOEP)Fe^{III}Br]^+$ obtained by oxidation of the preceding sample with 1 equiv of bromine. (B) Electronic spectra of the same sample after reduction with zinc and filtration. Cell path length: 1.0 mm.

already been established.[9] The ^1H NMR spectra of the iron(II) porphyrins **6–10** have been described and analyzed previously.[10]

The iron(III) *N*-alkylporphyrin complexes have received relatively little attention. Electrochemical studies indicate that the iron(II)/iron(III) couple is reversible.[6,7] Electronic spectra of electrochemically generated iron(III) *N*-phenylporphyrin complexes have been described.[6] Ogoshi and co-workers[11] have isolated stable salts of $[(MeOEP)FeCl]^+$ with $FeCl_4$ and ClO_4 counterions from the reaction of (MeOEP)H with iron(II) chloride and an unidentified oxidant. The magnetic susceptibility and ESR properties of these materials indicate that they have a high-spin ($S = {}^5/_2$) ground state.[11]

Results

Chemical oxidations have been performed in chloroform solutions by using the halogens chlorine, bromine, and iodine as oxidants. Under these conditions the iron(III) products exhibited limited stability, and consequently our observations were made at ca. −50 °C in order to retard the rate of product decay. We attribute the product loss in part to the presence of a nucleophilic anion that can cause dealkylation of the porphyrin (vide infra). Preliminary studies involved titrations of the iron(II) complexes with controlled amounts of oxidant. We found however that, after the addition of 1 equiv of bromine or chlorine, the addition of excess oxidant had no effect on the spectral features of the iron(III) complexes. With iodine as the oxidant it was necessary to employ an excess of oxidant. In all cases the oxidation can be reversed by treating the oxidized solution with zinc dust.

Electronic Spectral Studies. The results of treating (MeTPP)$Fe^{II}Br$ with bromine are shown in Figure 1. The solid line in Figure 1A shows the spectrum of green (MeTPP)$Fe^{II}Br$ before oxidation while the dotted line shows the spectrum of the red solution after the addition of 1 equiv of bromine. The dotted trace then is the spectrum of $[(MeTPP)Fe^{III}Br]^+$. The spectral changes are consistent with previous observations.[6,11] The Soret band has undergone a blue shift and has broadened upon oxidation. Additionally the intensity in the α and β regions has diminished. These changes are reversed when zinc dust is added the sample. Figure 1B shows the spectrum of the solution obtained after the sample was treated with zinc and then filtered. The reduction in spectral intensity in comparison to that of trace A results from some dilution that occurred during filtration.

Similar results involving the oxidation of (MeOEP)$Fe^{II}Br$ are shown in Figure 2. The spectrum of $[(MeOEP)Fe^{III}Br]^+$ shown in the dotted trace in part A is consistent with the spectrum of $[(MeOEP)Fe^{III}Cl]^+$ reported earlier.[11]

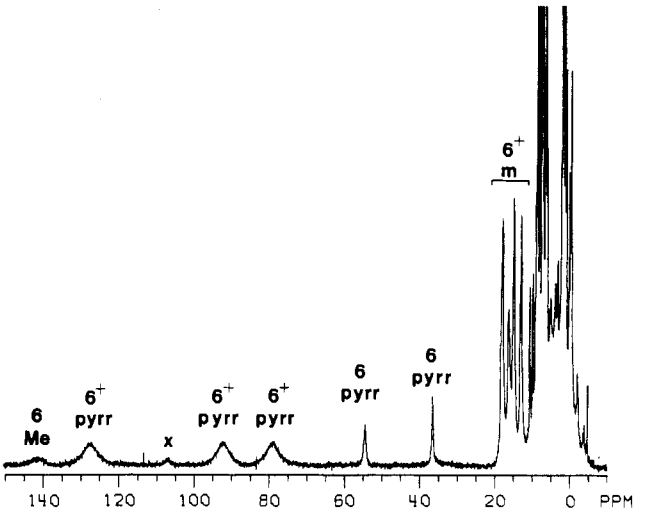

Figure 3. ^1H NMR spectrum of a chloroform-*d* solution at −50 °C of (MeTPP)$Fe^{II}Cl$ (**6**) to which less than 1 equiv of chlorine has been added. Resonances due to (MeTPP)$Fe^{II}Cl$ are labeled **6** and those of $[(MeTPP)Fe^{III}Cl]^+$ as $\mathbf{6}^+$; pyrr denotes pyrrole protons, Me denotes *N*-methyl protons, and m denotes meta phenyl protons.

NMR Studies. The NMR data have been analyzed on the presumption that the C_s geometry (**11**) of the iron(II) complexes[7] is retained upon oxidation. In this case there are four distinct

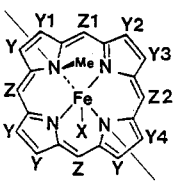

11

pyrrole positions, Y1–Y4, and two meso positions, Z1 and Z2. With phenyl rings in both of the two meso positions, it may be anticipated that the ortho and meta positions on each ring will be distinguishable due to the nearly perpendicular relationship between the phenyl plane and the plane of the adjacent pyrrole ring and the restricted rotation about the meso carbon–phenyl bond. For ethyl groups bound to the pyrrole sites, Y1–Y4, the methylene groups will be diastereotopic. Thus eight methylene hydrogen environments will be present while only four methyl environments are anticipated.

The effects of the addition of less than 1 equiv of chlorine to a solution of (MeTPP)$Fe^{II}Cl$ (**6**) are shown in the ^1H NMR spectrum in Figure 3. Separate resonances of **6** and its one-electron-oxidation product $\mathbf{6}^+$ are readily detected. Thus the rate of electron exchange between **6** and $\mathbf{6}^+$ is slow on the NMR time scale. We estimate the rate constant for exchange to be much

(9) La Mar, G. N.; Waker (Jensen), F. A. In "The Porphyrins"; Dolphin, D., Ed.; Academic Press: New York, 1979; Vol. 4, p 61.
(10) Balch, A. L.; Chan, Y. W.; La Mar, G. N.; Latos-Grazynski, L.; Renner, M. W. *Inorg. Chem.* **1985**, *24*, 1437.
(11) Ogoshi, H.; Kitamura, S.; Toi, H.; Aoyama, Y. *Chem. Lett.* **1982**, 495.

Table I. NMR Data for Iron(III) *N*-Methylporphyrin Halide Complexes

	chemical shifts, ppm (line widths, Hz)[a]			
	(TPP)$Fe^{III}Cl$	$[(MeTPP)Fe^{III}Cl]^+$ **6**$^+$	$[(MeTPP)Fe^{III}Br]^+$ **7**$^+$	$[(MeTpTP)Fe^{III}Cl]^+$ **8**$^+$
pyrrole	115	128 (1200)[b]	131 (500)	128 (1500)
		92 (1000)[b]	96 (460)	90 (1000)
		79 (1000)[b]	76 (480)	76 (1200)
m-H	16.5	17.4 (160)	20.1 (60)	18.8 (200)
	14.6	16.2 (280)	18.3 (60)	16.5 (170)
		14.8 (150)	17.2 (60)	15.5 (160)
		12.8 (150)	13.9 (60)	13.4 (150)
p-H	5	6.2 (70)	6.5 (28)	17.2 (60)[c]
		−0.4 (100)	−1.4 (30)	8.1 (50)[c]
N-methyl		272 (900)[d]		

[a] In chloroform-*d* solution at −50 °C. [b] ^2H NMR of deuterated-pyrrole **6**$^+$: 126 (160), 91 (150), 76 (140), 2.4 (140). [c] Methyl protons. [d] ^2H NMR data.

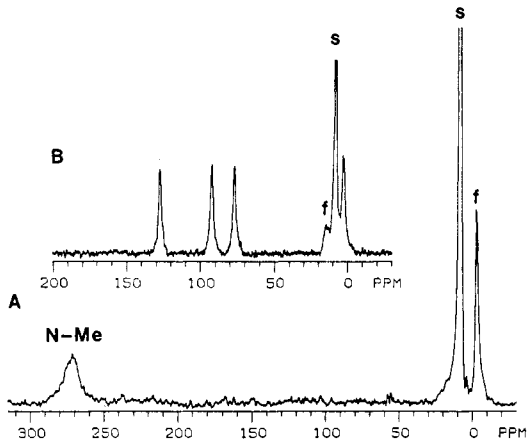

Figure 4. ^2H NMR spectra of chloroform solutions at −50 °C of $[(MeTPP)Fe^{III}Cl]^+$ (**6**$^+$) in which (A) the *N*-methyl group is deuterium labeled or (B) the pyrrole protons are deuterium labeled. The peaks labeled f result in part A from the deuterated methyl group of CD_3TPPH and in part B from the deuterated pyrrole protons of MeTPPH-d_8.

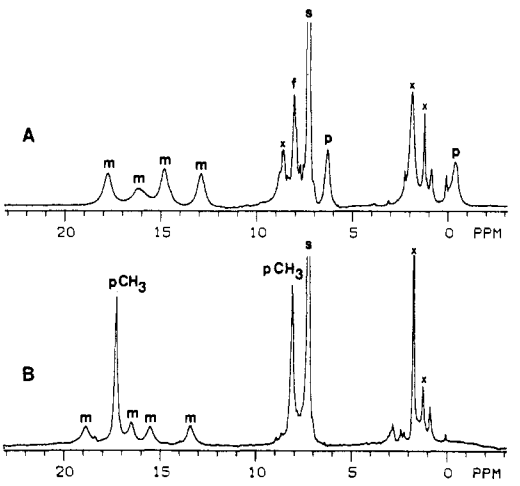

Figure 5. ^1H NMR spectra of chloroform-*d* solutions at −50 °C in the +20 to −3 ppm region of (A) $[(MeTPP)Fe^{III}Cl]^+$ and (B) $[(MeTpTP)Fe^{III}Cl]^+$. Peak labels: m, meta protons; p, para protons; pCH_3, para-methyl protons; s, undeuterated solvent; ×, impurities.

less than 6×10^4 s^{-1}. The resonances of **6** are labeled in accord with previously determined assignments.[10] The resonances of $[(MeTPP)Fe^{III}Cl]^+$ (**6**$^+$) consist of three broad resonances in the region 130–70 ppm and a group of four narrower resonances in the 20–10 ppm range. Other resonances in the crowded diamagnetic region 10–0 ppm are not readily picked out in this spectrum. The resonance assignments shown in Figure 3 and in Table I, where data for this and other new complexes are given, have been made on the basis of selective deuterium and methyl labeling.

In order to identify the pyrrole resonances, the ^2H NMR spectrum of $[(MeTPP\text{-}d_8)Fe^{III}Cl]^+$ generated from deuterated-pyrrole **6** (Y = D) has been obtained. It is shown in Figure 4, trace A. Four equally intense resonances are apparent, as indicated. Three of these correspond to the downfield resonances in Figure 3 while the 2.4 ppm resonance in Figure 4 is obscured in Figure 3. The *N*-methyl resonance has also been identified through ^2H NMR spectroscopy. The spectrum of $[(Me\text{-}d_3\text{-}TPP)Fe^{III}Cl]^+$ is shown in trace B of Figure 4. The broad resonance at 270 ppm is the *N*-methyl resonance. This feature does not appear in the ^1H NMR spectrum in Figure 3. Assuming a paramagnetic dipolar origin for the ^2H CD_3 line width over that of the ^2H pyrrole line width, the relative magnetogyric ratios predict a ^1H line width for *N*-CH_3 >10 kHz, well in excess of reasonably observable lines.

Figure 5 shows an expansion of the 20–0 ppm region of the ^1H NMR spectrum of $[(MeTPP)Fe^{III}Cl]^+$ (**6**$^+$) and compares it to the spectrum of $[(MeTpTP)Fe^{III}Cl]^+$ (**8**$^+$). This comparison clearly allows the two para proton and two para-methyl proton resonances to be identified. The four resonances of comparable width in the 20–10 ppm range are assigned to the meta phenyl protons. These resonances are all broader than those of para phenyl protons as expected due to their close proximity to the iron.

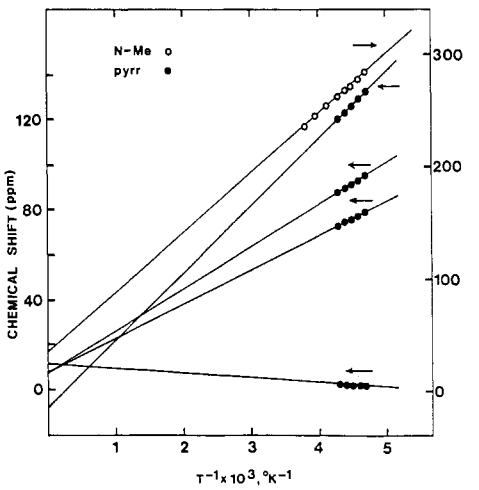

Figure 6. Curie plot for the *N*-methyl and pyrrole deuterium atoms in appropriately deuterated $[(MeTPP)Fe^{III}Cl]^+$.

The ortho phenyl proton resonances, which should be even broader, have not been detected. Presumably they lie under the resonances in the 3–0 ppm region.

Oxidation of $(MeTPP)Fe^{II}Br$ with bromine produces $[(MeTPP)Fe^{III}Br]^+$ (**7**$^+$), whose spectral features are given in Table I. The chemical shifts of all protons in **7**$^+$ differ from those of the chloro analogue **6**$^+$, so that at least one axial halide is coordinated after oxidation. Additionally, the line widths of all resonances decrease on going from $[(MeTPP)Fe^{III}Cl]^+$ to $[(MeTPP)Fe^{III}Br]^+$.

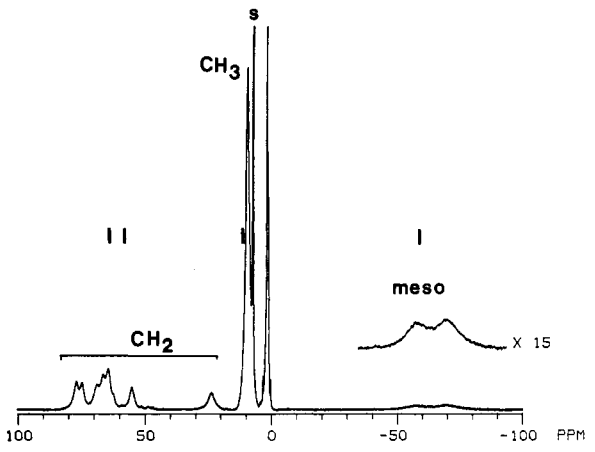

Figure 7. ^{1}H NMR spectrum of a chloroform-*d* solution at −50 °C of $[(MeOEP)Fe^{III}Cl]^+$. For comparison the bars show the resonance positions of the two methylene protons, the methyl protons, and the meso protons in $(OEP)Fe^{III}Cl$ at −50 °C.

$[(MeTPP)Fe^{III}Cl]^+$ and $[(MeTPP)Fe^{III}Br]^+$ are formed when $(MeTPP)Fe^{II}Cl$ and $(MeTPP)Fe^{II}Br$, respectively, are oxidized with an excess of iodine. However, when $(MeTPP)Fe^{II}Br$ is oxidized with chlorine or $(MeTPP)Fe^{II}Cl$ is oxidized with bromine, mixtures of $[(MeTPP)Fe^{III}Br]^+$ and $[(MeTPP)Fe^{III}Cl]^+$ are formed. In all of these experiments in which different halide ligands and halogen oxidants are employed, only two species, $[(MeTPP)Fe^{III}Br]^+$ and $[(MeTPP)Fe^{III}Cl]^+$, are observed. Consequently we conclude that only one halide ligand is coordinated in these iron(III) complexes. The other anion is present as an noncoordinating counterion.

A Curie plot for the *N*-methyl and pyrrole ^{2}H NMR resonances of $[(MeTPP)Fe^{III}Cl]^+$ is given in Figure 6. While the experimental data are consistent with linear behavior over the limited temperature range, the extrapolated intercepts are outside the normal diamagnetic positions, which have been estimated from the data for diamagnetic Zn(II) complexes.[10] Intercepts outside the normal diamagnetic positions are expected for high-spin iron(III) systems with significant zero-field splitting.[12-14]

Figure 7 shows the ^{1}H NMR spectrum of $[(MeOEP)Fe^{III}Cl]^+$ obtained by chlorine oxidation of $(MeOEP)Fe^{II}Cl$. The two broad (~3000-Hz half-width) upfield resonances at −63 and −75 ppm are assigned to the meso protons on the basis of their relative areas and comparable line widths. The resonances at 77, 75, 69, 66, 63, 62, 55, and 23 ppm are assigned to the eight distinct methylene protons. They have equal areas, each equivalent to two protons per molecule, and comparable line widths. The methyl resonances of the ethyl groups appear as a relatively narrow, undifferentiated resonance at 9.5 ppm. The *N*-methyl resonance was not detected, an observation that is consistent with our ^{1}H NMR results on $[(MeTPP)Fe^{III}Cl]^+$. Reduction of the solution that produced the spectrum in Figure 7 with zinc dust restored the ^{1}H NMR spectrum of $(MeOEP)Fe^{II}Cl$.

Electron Spin Resonance Spectra. The iron(II) complexes **6–10** do not exhibit ESR signals in frozen chloroform solution at −196 °C. Upon oxidation of $(MeTPP)Fe^{II}Cl$ with chlorine, an ESR spectrum ($g_\perp = 5.86$, $g_\parallel = 2.16$) characteristic of other five-coordinate, high-spin ($S = {}^5/_2$) iron porphyrins[15,16] is observed for the frozen chloroform solution. This spectrum is distinct from that of $(TPP)Fe^{III}Cl$ ($g_\perp = 5.66$, $g_\parallel = 2.03$, with a narrower line at 5.66 under identical conditions). Treatment of the ESR-active sample with zinc dust results in the loss of the ESR signal and restores the electronic spectrum of $(MeTPP)Fe^{II}Cl$. Treatment of $(MeTPP)Fe^{II}Br$ with bromine in chloroform followed by freezing at −196 °C produces a similar ESR spectrum ($g_\perp = 5.66$, $g_\parallel = 2.14$).

Sample Decomposition. Under the conditions used in this work the iron(III) complexes are unstable. The products resulting from this instability depend on the anion present. When chloroform solutions of $[(MeTPP)Fe^{III}Cl]^+$ (formed by chlorine oxidation of **6**) are warmed, NMR and electronic spectra indicate that demetalation occurs and *N*-methyltetraphenylporphyrin is released. Some evidence of this mode of decomposition occurring even at low temperature is present in the ^{2}H NMR spectra in Figure 4, where the peaks labeled f result from *N*-methyltetraphenylporphyrin. During decomposition an intermediate can be detected. At −30 °C this species has three pyrrole resonances (confirmed by ^{2}H NMR spectroscopy on a deuterated-pyrrole sample) at ~15 ppm. On cooling, these shift to higher fields thus displaying antiferromagnetic behavior. This species has also been detected as a minor product resulting from insertion of iron into *N*-methyltetraphenylporphyrin. However we have not been able to obtain a pure sample of the material. The antiferromagnetic behavior suggests that it is a dimeric species, possibly an oxo-bridged dimer analogous to the well-known $(TPP)FeOFe(TPP)$.

With $[(MeTPP)Fe^{III}Br]^+$ (formed by bromide oxidation of **7**), however, the principal products of decomposition are $(TPP)Fe^{III}Br$, which has been detected by both ^{1}H NMR spectroscopy and electronic spectroscopy, and methyl bromide, which produces a characteristic NMR resonance at 2.4 ppm that grows as the sample decomposes. The preference for demethylation in the latter case can be attributed to the higher nucleophilicity of bromide vs. chloride.

Addition of *N*-methylimidazole (*N*-MeIm) also induces the decomposition of $[(MeTPP)Fe^{III}Cl]^+$. The products are *N*-methyltetraphenylporphyrin, and a paramagnetic iron/*N*-MeIm complex.

Discussion

The spectroscopy results are all in accord with a high-spin ($S = {}^5/_2$) electronic structure for these iron(III) complexes. The basic C_s symmetry of the iron(II) complexes is retained upon oxidation.

The NMR spectra clearly display characteristics that reveal the lowering of symmetry that N-methylation produces. Nevertheless, the pattern of chemical shifts for these iron(III) species resembles that of symmetrical high-spin iron(III) porphyrins.[12-14] A comparison of the spectra of $(TPP)Fe^{III}Cl$ and $[(MeTPP)Fe^{III}Cl]^+$ in Table I reveals that three of the pyrrole resonances of the latter occur near the pyrrole position for $(TPP)Fe^{III}Cl$. Likewise the meta phenyl and para phenyl proton resonances appear in similar regions for both species. Turning to Figure 7, one can see that the chemical shifts for $[(MeOEP)Fe^{III}Cl]^+$ and $(OEP)Fe^{III}Cl$ fall into similar ranges. The bars above the spectrum give the extrapolated resonance position for $(OEP)Fe^{III}Cl$ at −50 °C. Additionally, the line widths in these iron(III) complexes and in their symmetrical high-spin iron(III) porphyrin counterparts show similar dependence on the coordinated halide. That is, the line widths decrease significantly on going from chloride to bromide. For such complexes the line width (δ) is related to the zero-field splitting parameter D ($\delta \propto D^{-2}$), and D is known to decrease from Br to Cl from a variety of spectroscopic observations.[13]

Depite these similarities between spectra, there are characteristic, informative differences. Clearly the lowering of symmetry and the very low-field shift of the *N*-methyl resonance are among these. The *N*-methyl resonance with its large downfield shift offers a distinctive characteristic for these iron(III) complexes. However its extreme breadth limits its observability and dictates that ^{2}H NMR be used to detect it. The downfield shift of this resonance is similar to that of many *N*-alkyl groups in paramagnetic complexes and reflects a σ-spin-transfer mechanism.[17,18]

Another characteristic feature of the iron(III) complexes is the localized effect of the *N*-methyl group on one pyrrole ring. For

(12) Walker, F. A.; La Mar, G. N. *Ann. N.Y. Acad. Sci.* **1973**, *206*, 328.
(13) La Mar, G. N.; Walker, F. A. *J. Am. Chem. Soc.* **1973**, *95*, 6950.
(14) La Mar, G. N.; Walker, F. A. *J. Am. Chem. Soc.* **1975**, *97*, 5103.
(15) Peisach, J.; Blumberg, W. E.; Ogawa, S.; Rahmilewitz, E. A.; Oltzik, R. *J. Biol. Chem.* **1971**, *246*, 3342.
(16) Cheng, R. J.; Latos-Grazynski L.; Balch, A. L. *Inorg. Chem.* **1982**, *21*, 2412.
(17) Fitzgerald, R. J.; Drago, R. S. *J. Am. Chem. Soc.* **1968**, *90*, 2523.
(18) Del Gaudio, J.; La Mar, G. N.; *J. Am. Chem. Soc.* **1978**, *100*, 1112.

$[(MeTPP)Fe^{III}X]^+$ one pyrrole resonance is clearly distinct from the other three and shows a considerable upfield shift. Likewise in $[(MeOEP)Fe^{III}Cl]^+$ there are two methylene resonances (at 55 and 23 ppm) that are shifted upfield so that they are set apart from all others.

The logical conclusion that follows is that N-methylation primarily affects spin transfer to the modified pyrrole ring. This leads to sharply decreased shifts for both the pyrrole protons and methylene groups of that modified ring. The three "normal" pyrrole rings exhibit proton and methylene shift patterns that are similar to those found for symmetrical, five-coordinate, high-spin iron(III) porphyrins. The similarity of the two meso-proton shifts in $[(MeOEP)Fe^{III}Cl]^+$ to those of $(OEP)Fe^{III}Cl$ again indicates that the porphyrin molecular orbitals, particularly the π orbitals, are largely intact and that the difference in shift patterns between $(TPP)Fe^{III}Cl$ or $(OEP)Fe^{III}Cl$ and $[(MeTPP)Fe^{III}Cl]^+$ or $[(MeOEP)Fe^{III}Cl]^+$ originates primarily in sharply attenuated σ-spin transfer to the methylated pyrrole as a consequence of the longer Fe–N distance tilting of the pyrrole ring out of the porphyrin plane and change in nitrogen hybridization.

Experimental Section

Chloroform-*d* (Aldrich) was dried over 4-Å molecular sieves before use. Samples of the iron(II) porphyrins **6**–**10** and the deuterated derivatives were prepared by established procedures, which we described and acknowledged previously.[10]

Oxidation Procedures. Solutions of known concentrations (ca. 1 mM for NMR, 0.1 mM for electronic spectroscopy) of the iron(II) complexes **6**–**10** were prepared in chloroform-*d* and cooled to ~−50 °C in a dry ice/acetonitrile bath. Solutions of known concentrations of the halogen oxidant in chloroform were then transferred with a glass pipet into the cold sample of the iron(II) complex. Addition was performed slowly to minimize warming of the sample. The cold samples were then transferred to the appropriate spectrometer for measurements.

Instrumentation. NMR spectra were recorded on a Nicolet NT-360 FT spectrometer (for 360-MHz ^1H NMR spectra) or a Nicolet NT-500 FT spectrometer (for 76.7-MHz ^2H NMR spectra) operating in the quadrature mode. Between 200 and 1000 transients were accumulated over a 40-kHz bandwidth with 16K data points for ^1H NMR (4–8K for ^2H NMR) and a 6-μs 90° pulse. The signal-to-noise ratio was improved by apodization of the free-fraction decay, which introduced a negligible 3–10 Hz of line broadening. Line widths were determined for nonoverlapping peaks by using the Nicolet computer subroutine LF, which fit the peaks to a Lorentzian line. Overlapping peaks were fit with the NTCCAP routine. The line broadening introduced by apodization was subtracted from the line widths. The peaks were referenced against tetramethylsilane. Electronic spectra were measured with a Hewlett-Packard 8450 A spectrophotometer or with a Cary 17 spectrophotometer equipped with a Kontes low-temperature optical cell and Dewar. Electron spin resonance spectra were recorded on a Varian E3 spectrometer.

Acknowledgment. We thank the National Institutes of Health (Grant GM26226) for financial support. L.L.-G. was on leave from the Institute of Chemistry, University of Wroclaw, Wroclaw, Poland.

Registry No. **6**, 64813-94-1; **6**$^+$, 96760-81-5; **7**, 95675-69-7; **7**$^+$, 96760-82-6; **8**, 95675-71-1; **8**$^+$, 96760-83-7; **9**, 95675-73-3; **9**$^+$, 82057-14-5; **10**, 95675-74-4; **10**$^+$, 96791-12-7.

Contribution from the Department of Chemistry,
Montana State University, Bozeman, Montana 59717

Proton Transfer and Ligand Displacement Reactions of Nickel(II) *N,N'*-Bis(2-aminoethyl)oxaldiamide

KIM E. GILMORE and GORDON K. PAGENKOPF*

Received December 11, 1984

The transfer of Ni(II) from *N,N'*-bis(2-aminoethyl)oxaldiamide, $NiH_{-2}ODEN$, to triethylenetetramine proceeds through three general routes. One of these is a dissociative path, $k_{H_2O} = 0.001\ s^{-1}$. Another is a proton-dependent pathway that involves adding a proton, $K = 6.1 \times 10^6\ M^{-1}$, followed by dissociation, $k_2 = 0.035\ s^{-1}$, or reaction with another proton, $7.0 \times 10^3\ M^{-1}\ s^{-1}$. The third route involves the replacing ligand and provided steady-state rate constant ratios, $k_{HT}/k_T = 0.25$ and $k_{H_2T}/k_T = 0.18$. The steady-state formation constant was $0.7\ s^{-1}$. The mechanism observed for EDTA is similar except in the magnitude of the EDTA-dependent constants. The steady state formation constant is less, $0.038\ s^{-1}$, and the ratio for the species is $k_{H_2Y}/k_{HY} = 35$. When the first proton adds, it is believed to form a five-membered ring.

Complexation of nickel(II) by *N,N'*-bis(2-aminoethyl)oxaldiamide is similar in several coordination sites to that obtained by other polypeptide ligands. Sketch I of the complex demonstrates the orientation of the donors and the chelate rings.[1] All three of the chelate rings are five-membered, and the negative charge is concentrated on one side of the low-spin yellow complex. This complex is similar to several complexes through elemental composition of the chelate rings. For example, it is similar to $NiH_{-2}MBAE$ since both have the amide group in the interior chelate ring.[2] It is also similar to $NiH_{-2}DGEN$ by having terminal coordination[3] of $-NH_2$.

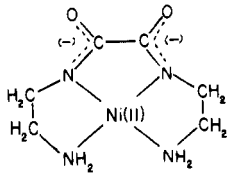

I, $NiH_{-2}ODEN$

This complex was reacted with triethylenetetramine and ethylenediaminetetraacetate over a sizable pH range. Similar reactions have studied the transfer of nickel(II) from triglycine,[4,5] diglycylamide,[6] tetraglycine,[7] and glycylglycylhistidine.[8] The reactions of $NiH_{-2}ODEN$ with the two displacing ligands proceed through a variety of parallel paths that may include protonated intermediates.

Experimental Section

The nickel stock solution, 0.100 M, was prepared from twice recrystallized $Ni(ClO_4)_2$ and was standardized by EDTA titration. Twice recrystallized $NaClO_4$ was used to maintain the ionic strength at 0.10 M for the kinetic runs. The trien stock solution was prepared from the twice recrystallized sulfate salt and standardized spectrophotometrically (575 nm) with use of standard copper(II). Primary standard Na_2EDTA was utilized. The ODEN ligand was synthesized by the Hill and Raspin method.[1] The nickel–ODEN complexes were prepared just before the

(1) Hill, H. A. O.; Raspin, K. A. *J. Chem. Soc. A* **1968**, 3036.
(2) Storvick, J. P.; Pagenkopf, G. K., submitted for publication in *Inorg. Chem.* 1984.
(3) Storvick. J. P.; Pagenkopf, G. K. *Inorg. Chem.*, in press.
(4) Bannister, C. E.; Margerum, D. W. *Inorg. Chem.* **1981**, *20*, 3149.
(5) Brice, V. T.; Pagenkopf, G. K. *J. Chem. Soc., Chem. Commun.* **1974**, *75*.
(6) Mason, C. F. V.; Chamberlain, P. I.; Wilkins, R. G. *Inorg. Chem.* **1971**, *10*, 2345.
(7) Paniago, E. B.; Margerum, D. W. *J. Am. Chem. Soc.* **1972**, *94*, 6704.
(8) Bannister, C. E.; Raycheba, J. M. T.; Margerum, D. W. *Inorg. Chem.* **1982**, *21*, 1106.

0020-1669/85/1324-2436$01.50/0